Regional SST and SLP conditions related to tornado 'outbreak' environments 15 days later

Zoe Schroder[1,1*]

[1*]Department of Applied Aviation Sciences, Embry-Riddle Aeronautical University, 1 Aerospace Boulevard, Daytona Beach, 32114, FL, United States of America.

Corresponding author(s). E-mail(s): schrodez@erau.edu;

Abstract

Global climate features are known to influence tornado frequency and convective environments in the US. However, current research does not quantify the relationship between climate variables and environmental factors at the scale of an outbreak. Here, the author quantifies the conditional relationships between precursor sea surface temperatures and sea level pressure variables and localized extremes of convective available potential energy and shear associated with clusters of ten or more tornadoes. To do this, the author fits linear regressions to global climate variables averaged over the fifteen days before the outbreak. The fifteen day averages prior to the cluster help estimate the changes in convective available potential energy and shear on days with at least ten tornadoes. Results show that for every 1° C increase in the sea surface temperature gradient between the Gulf of Alaska and the Caribbean, deep-layer bulk shear increases by 0.88 m s^{-1}, shallow-layer bulk shear increases by 0.62 m s^{-1}, and convective available potential energy decreases by 50.6 J kg^{-1}, conditional on at least ten tornadoes, and holding the other variables constant. This result highlights the role of the thermal wind on environmental factors that influence clusters with at least ten tornadoes. Further, model results show that for every 1° E increase in longitude of the cluster centroid, deep-layer bulk shear increases by 0.15 m s^{-1}, shallow-layer bulk shear increases by 0.38 m s^{-1}, and convective available potential energy decreases by 39.3 J kg^{-1}, conditional on at least ten tornadoes, and holding the other variables constant. Model results remain

consistent with the work of others who highlight increased CAPE in the Great Plains and increased shear in the Southeast. Additionally, shallow-layer bulk shear is the only environmental factor that has a significant upward annual trend which could lead to increased tornado activity.

Keywords: Climate Change, Tornado Outbreak, CAPE, shear, linear mixed-effect models

** This manuscript is currently In-Review with the Journal of Theoretical and Applied Meteorology. **

Introduction

Tornado outbreaks are severe convective events characterized by many tornadoes over a confined spatial area with the potential for destruction and casualties (Elsner et al, 2015; Fuhrmann et al, 2014; Dean and Schneider, 2012; Schneider et al, 2004; Mercer et al, 2009; Galway, 1977). On average, tornado days are declining annually (Elsner et al, 2015; Moore, 2017, 2018; Moore and DeBoer, 2019). However, the number of tornadoes and accumulated tornado power (ATP) on these days in on the rise (Schroder and Elsner, 2021; Elsner et al, 2015; Tippett et al, 2016; Moore, 2017; Tippett and Cohen, 2016; Moore, 2018; Elsner et al, 2018; Moore and DeBoer, 2019; Schroder and Elsner, 2019). Convective available potential energy (CAPE), shallow-layer bulk shear (SLBS; 1000 hPa to 850 hPa), and deep-layer bulk shear (SLBS; 1000 hPa to 500 hPa) are environmental factors that significantly influence tornado and casualty counts and ATP in outbreaks with at least ten tornadoes (Schroder and Elsner, 2021, 2019; Elsner et al, 2018, 2013).

Environmental factors for severe convective weather will increase in the future (DelGenio et al, 2007; Trapp et al, 2007; Hoogewind et al, 2017; Seeley and Romps, 2015b; Diffenbaugh et al, 2008; Brooks, 2013; Seeley and

Romps, 2015a). Currently, large CAPE values coincide with areas where moisture advection is minimal relative to the southeastern US, where CAPE values are much smaller (Marsh et al, 2007; Gensini and Mote, 2015). Rising surface temperatures lead to an increase in CAPE values (Elsner et al, 2014; DelGenio et al, 2007; Hoogewind et al, 2017; Brooks, 2013; Trapp et al, 2007; Elsner et al, 2018) and decrease in bulk shear (BS) as a result of the weakened temperature gradient between the equator and the poles (Brooks, 2013; Diffenbaugh et al, 2008). The projected decrease in BS is smaller than the projected increase in CAPE leading to an increased frequency of favorable convective environments (DelGenio et al, 2007; Trapp et al, 2007; Brooks, 2013; Hoogewind et al, 2017). Research identifies increasing favorable convective environments in the Midwest and Northeast with little to no change in the frequency of favorable environments in the SoutheastGensini et al (2013).

Large-scale climate features, such as increased surface temperatures, sea surface temperatures (SST), and phases of global wind patterns influence tornado frequency and favorable convective environments in the US. Research shows that the North Atlantic Oscillation (NAO), Pacific North American (PNA), Madden-Julian Oscillation (MJO), and El-Nino Southern Oscillation (ENSO) influence environmental conditions over the US (Elsner et al, 2016b; Chu et al, 2019; Allen et al, 2015a; Lee et al, 2013, 2016; Marzban and Schaefer, 2001; Tippett et al, 2015; Cook et al, 2017; Gensini et al, 2019; Baggett et al, 2018). For example, the phase of the NAO dictates the strength of the westerly winds and pressure gradient over the Atlantic, which can lead to an increase (positive phase) or decrease (negative phase) in tornado probability (Elsner et al, 2016b). The phase of the PNA also dictates weather patterns in the US through the strength and location of the East Asian jet stream (Chu et al, 2019). The phase of the ENSO directly influences tornado frequency by

modulating the polar and subtropical jet streams (Allen et al, 2015a; Lee et al, 2013, 2016; Marzban and Schaefer, 2001; Tippett et al, 2015; Cook et al, 2017). Alternatively, the Madden-Julian Oscillation (MJO) is a tropical zone of convection that propagates along the equator over 30 to 60 days (Gensini et al, 2019). However, the amplitude and location of the convection increases the predictive lead time for convective environments by 2 to 5 weeks Baggett et al (2018). Although these relationships are extensively related to tornado frequency and favorable convective environments, limited research has quantified the relationship between these large-scale climate features and environmental factors that are known to influence tornadoes at the scale of an outbreak.

The goal of this paper is to determine which large-scale climate variables precede tornado clusters in the US. I define a cluster as a group of tornadoes with at least ten tornadoes on a single convective day (24-hour period; 1200 UTC to 1200 UTC). I am interested in the regional SST and sea level pressure (SLP) conditions fifteen days before a cluster occurs. However, I am not examining whether these precursor conditions can anticipate the occurrence of a cluster. Instead, I address the following question: Given a cluster, what regional SST and SLP patterns fifteen days prior are statistically and physically related to the amount of CAPE and shear associated with the cluster?

The study quantifies the conditional relationships between precursor SST and SLP variables and local extremes of CAPE and shear associated with large outbreaks. First, I assign each global climate variable to its respective cluster in section 2. Then, I highlight the descriptive statistics for the clusters in the data in section 3. Next, I fit a series of regression models to cluster-level environmental data and climate variables on convective days when the number of tornadoes is at least ten in section 4 [see (Schroder and Elsner, 2019)]. I provide a discussion of the results in section 5. Finally, the conclusions are in section 6.

Data and Methods

This section includes a description of the data collation process, organization, and procedures to aggregate values to the cluster level. For this research, I define a cluster as a group of at least ten tornadoes that occur relatively close together in both space and time during a single convective day. I select ten as the cut-off value because it is often used to formally define an outbreak (Galway, 1977; Anderson-Frey et al, 2018). Additionally, a selection of ten tornadoes helps alleviate uncertainty caused by too few clusters and excessive time to fit models caused by too many clusters (Elsner and Schroder, 2019).

Tornado Clusters

I download tornado data from the Storm Prediction Center (SPC; https://www.spc.noaa.gov/gis/svrgis/). I extract the date, time, and genesis location for all tornado reports between 1994 and September 2020. The year 1994 is selected as the start of analysis because it is the first year of the extensive use of the WSR-88D weather radar (Heiss et al, 1990). During this time frame, there are a total of 33,143 tornado reports. I convert the geographic coordinates for each genesis location to Lambert conic conformal coordinates, where the projection is centered on 96° W longitude.

I compute the sum of the space and time distances between the genesis locations for each tornado. This results in a single value for each tornado's space-time distance. Next, I assign each tornado a cluster identification number based on the space-time distance. I assign two tornadoes the same cluster number if they occur close together in space and time. Clustering ends when the difference between the individual tornado and existing clusters surpasses 50 000 s (roughly 14 hours). Then, I divide the space-time difference by 15 m s^{-1} to account for the average speed of tornado-producing storms, which

is commensurate with the magnitude of the steering-level wind field. Additional detail about the clustering procedure, along with a comparison of the resulting clusters to well-known outbreaks, is available in Schroder and Elsner (2019) (Schroder and Elsner, 2019). This method produces an 80% match with the operational methodology outlined in Gensini et al. (2020) indicating a successful algorithm (Gensini et al, 2020).

I select only clusters with at least ten tornadoes occurring within the same convective day. In total, there are 830 clusters with a total of 18 571 tornadoes used in this research. The average number of tornadoes per cluster is 22, with a maximum of 173 (27 April 2011). The clusters have a right-skewed distribution, with 88 clusters containing exactly ten tornadoes. The minimum convex hull (black polygon) that includes all tornado genesis locations defines the cluster area. Figure 1 is an example of the May 20, 2019, cluster. This day had a total of 49 tornadoes that occurred over Oklahoma and Texas. It had an area of 155 338 km^2 and lasted roughly 17 hours. It resulted in a total of 4 casualties (sum of injuries and fatalities).

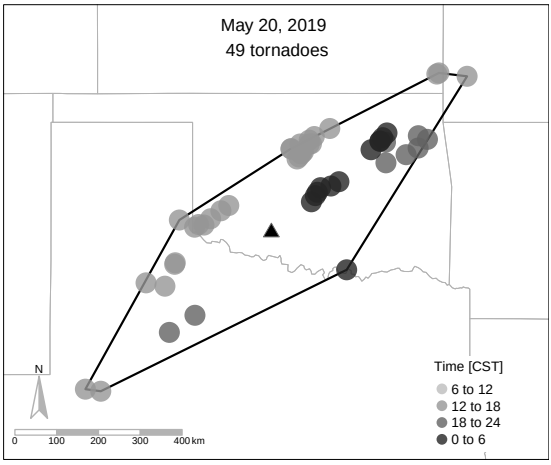

Fig. 1 Example of a cluster in the tornado dataset. The solid black line is the minimum convex hull that contains all tornadoes in this cluster. Each circle is a tornado genesis location. The grayscale represents the time that each tornado occurred. The black triangle is the centroid of this cluster.

There were cases where multiple clusters occurred on the same day. Although these clusters may result from the same synoptic system, I do not group them together because the minimum tornado space-time distance exceeds the threshold value. In this research, I do not attempt to identify the system that produced these tornadoes and use the term cluster instead of outbreak.

Environmental Factors

CAPE, BS, and weak convective inhibition (CIN) are large-scale environmental factors known to influence tornado development (Rasmussen and Blanchard, 1998; Thompson et al, 2003; Shafer and Doswell, 2011; Doswell et al, 2006). I obtain the environmental factors from the National Centers for Atmospheric Research's North American Regional Reanalysis (NARR) (Mesinger et al, 2006). The horizontal grid spacing of NARR is 32 km. All NARR values are available in 3-hour increments beginning at 0000 UTC. In the severe convective weather literature, researchers often refer to these environmental factors as "parameters." Here, I refer to them as factors since the term "parameter" denotes an unknown coefficient in statistical modeling methodology, which is employed here.

For each cluster, I select the nearest 3-hour NARR time before the occurrence of the first tornado. For example, I select the 1200 UTC environmental factors for a cluster whose first tornado occurs at 1347 UTC. The NARR time before the start of each cluster allows the data to be less contaminated by deep convection. However, this choice can lead to underestimating the severity of environmental factors when environments conducive to tornadogenesis are rapidly changing. In total, about 57% of all clusters have an initial tornado

between 18 UTC and 00 UTC. However, there are more tornadoes in clusters when the first tornado occurs between 18 UTC and 21 UTC on average.

The environmental factors considered in this research include CAPE (0-180 hPa above ground level), DLBS (1000 - 500 hPa), and SLBS (1000 - 850 hPa). I calculate the shear variables as the square root of the sum of the squared differences between the u- and v- wind components at the respective levels consistent with others (Tippett et al, 2012). Climate researchers often use these specific variables as proxies for more traditional variables used to forecast severe convective weather (Allen et al, 2015b; Moore et al, 2016; Tippett et al, 2012; Schroder and Elsner, 2019; Elsner and Schroder, 2019; Schroder and Elsner, 2021).

For each environmental variable, I select the highest value across the raster grid confined within the area defined by the cluster's convex hull to represent the cluster (Fig. 2). I select the maximum value to capture environments unaltered by deep convection as a result of tornadogenesis. I do not use the mean value because the tornado and non-tornado producing convection within the cluster's convex hull often influence the environmental factors. Histograms (not shown) of the maximum values show no evidence of extreme behavior.

I do not include storm-relative helicity (SRH), lifted condensation level (LCL), and dewpoint temperature (DEW) in this research, although proven to indicate favorable environments for tornadogenesis. Eliminating these environmental factors is consistent with other researchers (Schroder and Elsner, 2021) who eliminate these variables as a result of the correlation to the other environmental factors such as CAPE, DLBS, and SLBS. Additionally, I do not use composite parameters, including the significant tornado parameter (STP) and supercell composite parameter (SCP) in this study. Gensini and de Guenni (2019) find that STP is a statistically significant covariate of tornado frequency

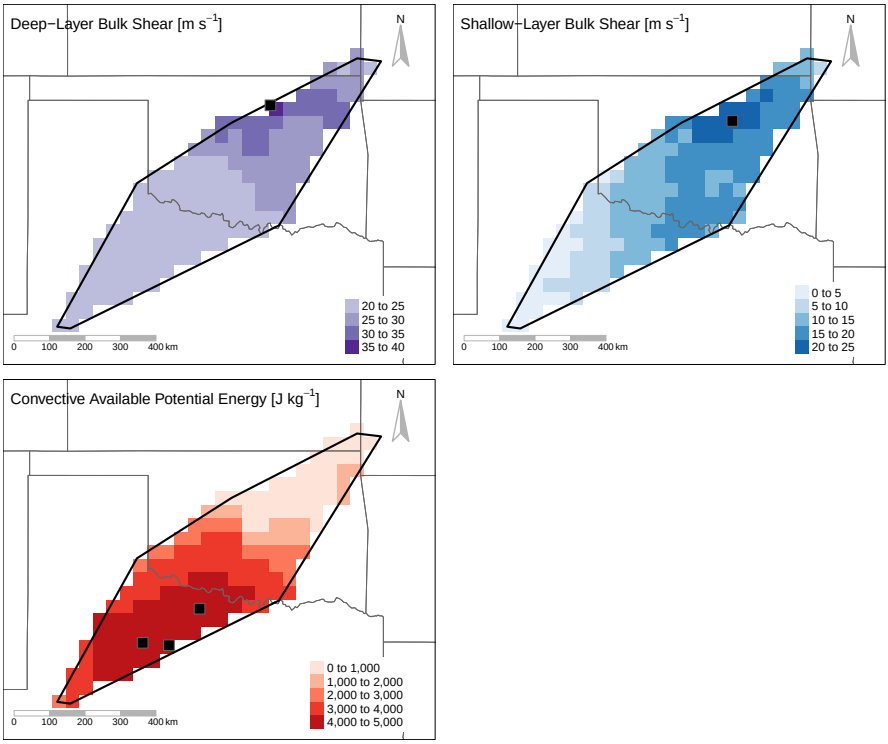

Fig. 2 Example of CAPE, DLBS, and SLBS for May 20, 2019. The black line is the spatial extent of the cluster. The color shading represents the intensity of the environmental factors. CAPE is red, DLBS is purple, and SLBS is blue. The black square is the location of the maximum value for the environmental factor. For the CAPE example, the maximum value occurred in three different locations indicated by the three black squares.

at the appropriate space-time scales (Gensini and Bravo de Guenni, 2019). However, STP and SCP are multiplicative variables that use CAPE and shear to calculate these variables. Therefore, the value of these composite variables could be a result of high CAPE and low shear or low CAPE and high shear. In this research, my focus is on the individual environmental factor as opposed to composite variables which use a combination of environmental factors in their calculations.

Climate Variables

This research leverages climate variables to statistically explain changes in CAPE, DLBS, and SLBS for the clusters. SSTs, NAO, PNA, and MJO represent the climate variables in this research because I influence tornado frequency in the US. A single daily average value is obtained for each of the fifteen days before the cluster for each climate factor. I compute the fifteen-day average for each climate variable per cluster by averaging the fifteen individual daily average. These variables were tested over several temporal averages including 5, 10, 15, 20, and 30 days. Each of these variables and their variety of averages are highly correlated with values greater than 0.79. Additionally, the 15-day average values significantly improve the models relative to the other averages. Therefore, I select the 15-day average value of the climate variables preceding the clusters.

Sea Surface Temperatures

I collect SST data from the High-Resolution Blended Analysis through the National Oceanic and Atmospheric Administration's (NOAA) Physical Sciences Laboratory. It contains information on the daily mean SST from September 1981 to the present. This research uses SSTs in three separate zones: the Caribbean, Gulf of Alaska, and the El Nino 3.4 region (Fig. 3). I select these zones because I have been used to understand tornado events in the US (Elsner and Widen, 2014; Forbes, 2006; Elsner et al, 2016b,a). The first SST zone in this study is the Caribbean SSTs (CSST) which extends from 90° W to 70° W and 15° N to 25° N (blue rectangle in Fig. 3). The second SST zone in this study is the Gulf of Alaska SSTs (GAKSST) which extends from 157.5° W to 133.1° W and 50.5° N to 60° N (green rectangle in Fig. 3).

Elsner and Widen (2014) found that tornado frequency decreases for increasing CSSTs and GAKSSTs (Elsner and Widen, 2014). The final SST zone in this study is the El Nino 3.4 (NinoSST) region which extends from 170° W to 120° W and -5° S to 5° N (yellow rectangle in Fig. 3). I average the SSTs in this region to obtain the value of the NinoSST. I select the NinoSST instead of the well-known El Nino 3.4 Index because the index is a 5-month average value. The average NinoSSTs for each region better represent the daily to weekly timescales in this research. NinoSSTs are known to influence tornado development.

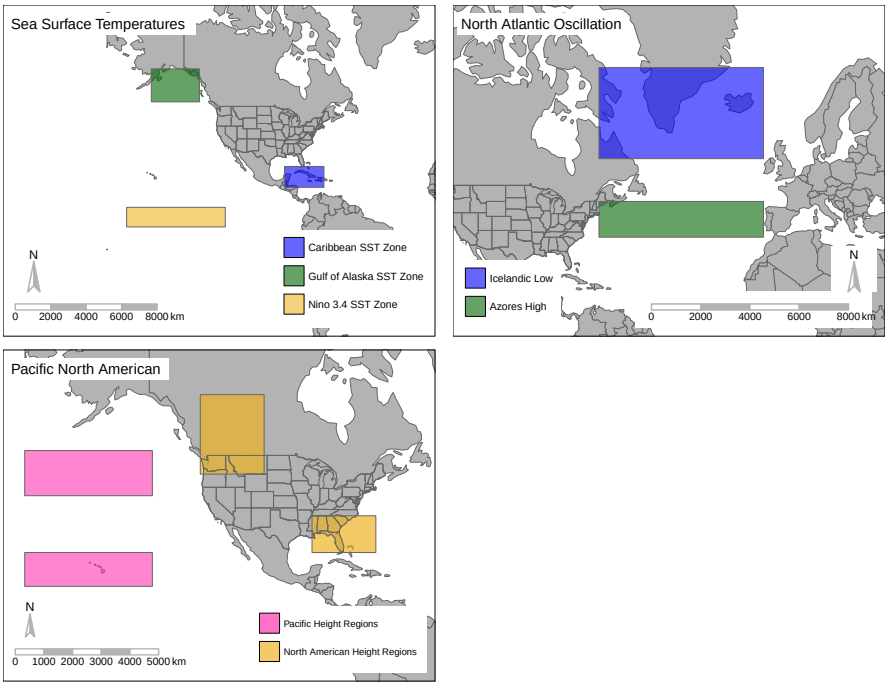

Fig. 3 The first panel highlights the SST zones used in this research. The blue rectangle is the extent of the CSST zone. The green rectangle is the GAKSST zone. The yellow rectangle is the NinoSST zone. The second panel highlights the regions used to calculate the NAO Index. It is calculated by taking the difference in the 500 hPa height patterns from the Azores High (green rectangle) and the Icelandic low (blue rectangle). The third panel highlights the regions used to calculate the PNA Index. The PNA is calculated as the difference between the difference in the 500 hPa height patterns for the two Pacific Regions (pink rectangles) and again for the two North American height regions.

North Atlantic Oscillation

I collect the NAO data from NOAA's Physical Science Laboratory (https://psl.noaa.gov/data/timeseries/daily/NAO/). The data set contains information on the daily value of the NAO Index from 1948 to the present. The index is calculated by taking the difference in the 500 hPa height patterns from the Azores High [35-45°N, 70-10°W] and Icelandic Low [55-70°N, 70-10°W] (see Fig. 3). The NAO values are standardized by the standard deviation of the monthly NAO index.

Pacific North American

I collect the PNA data from NOAA's Physical Science Laboratory (https://psl.noaa.gov/data/timeseries/daily/PNA/). The data set contains information on the daily value of the PNA Index from 1948 to the present. The index is calculated by taking the difference between the 500 hPa height patterns between northern Pacific Ocean [40-50°N, 180-140°W] and southern Pacific Ocean [15-25°N, 180-140°W] and northern North America [45-60°N, 125W-105°W] and southern North America [25-35°N, 90W-70°W] (see Fig. 3).

Madden-Julian Oscillation

I collect the MJO data from NOAA's Physical Science Laboratory through the Australian Bureau of Meteorology (http://www.bom.gov.au/climate/mjo/graphics/rmm.74toRealtime.txt). For this research, the MJO is the amplitude of the wave pattern. Strong amplitudes of MJO indicate enhanced convection along the equator. The temporal range of the MJO extends from weekly to monthly timescales. It is most known for its influence on the strength of global monsoon patterns, variations in wind and precipitation, and hurricanes.

Descriptive Statistics

DLBS does not have a significant diurnal variation but does have a seasonal pattern (Fig.4). The propagation of the polar jet stream during the winter lends itself to increased DLBS values (Sherburn and Parker, 2014; Sherburn et al, 2016). DLBS values decrease during the summer months when the polar jet stream retreats northward (Cheng et al, 2015). The seasonal variability of DLBS must be taken into account when fitting a model to estimate DLBS using climate variables.

The values of maximum DLBS follow a normal distribution (Fig. 5a) with a maximum value of 47.9 m s^{-1} and a minimum value of 5.59 m s^{-1} for clusters with at least ten tornadoes (Table 1). The median value of DLBS is 27.6 m s^{-1}. The mean value of DLBS in clusters with more than ten tornadoes is 27.6 m s^{-1}. In total, 50.1 % of clusters have less than the mean value of DLBS.

SLBS does not have a significant diurnal variation but does follow a seasonal pattern consistent with DLBS (Fig.4). Similar to DLBS, the propagation of the polar jet stream directly influences the values of SLBS (Sherburn and Parker, 2014; Sherburn et al, 2016).

The values of maximum SLBS follow a normal distribution (Fig. 5b). The maximum value of SLBS is 35.7 m s^{-1} with a minimum value of 1.08 m s^{-1} for clusters with at least ten tornadoes (Table 1). The median value of SLBS is 15.1 m s^{-1}. The mean value of SLBS for clusters with at least ten tornadoes is 15.2 m s^{-1}. In total, 51.8% of clusters have less than the mean value of SLBS.

CAPE follows both a diurnal and seasonal pattern (Fig.4). During the summer months, CAPE values increase as a result of increased air temperatures (Cheng et al, 2015). These larger CAPE values indicate more buoyant air leading to a greater potential for convection to occur. Additionally, CAPE follows a diurnal pattern. CAPE values are highest in the afternoon and early evening

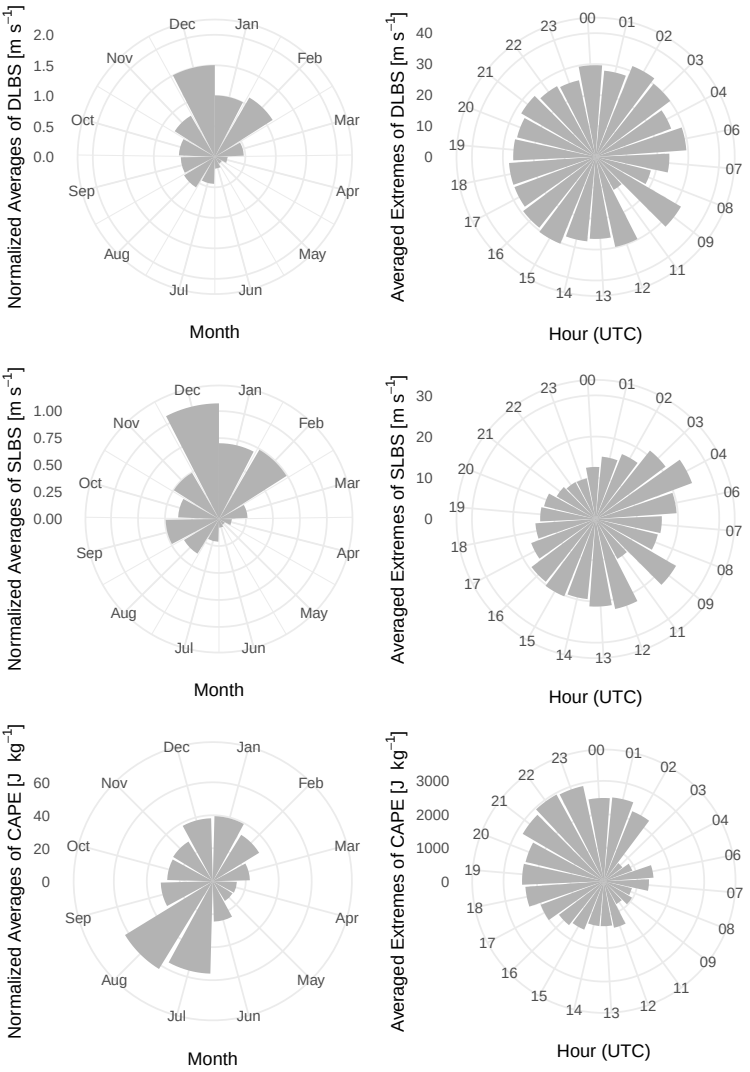

Fig. 4 Monthly and Hourly variability of DLBS (top row), SLBS (middle row), and CAPE (bottom row) for clusters with at least ten tornadoes. The month (left column) is normalized by the total number of clusters in each month. The hour (right column) is the average of the extreme values of the environmental factors.

hours when the daily temperatures are warmest, and CAPE values are lowest during nocturnal events (Sherburn and Parker, 2014).

The values of maximum CAPE do not follow a normal distribution (Fig. 5c). The maximum value of CAPE is 6530 J kg^{-1} with a minimum value

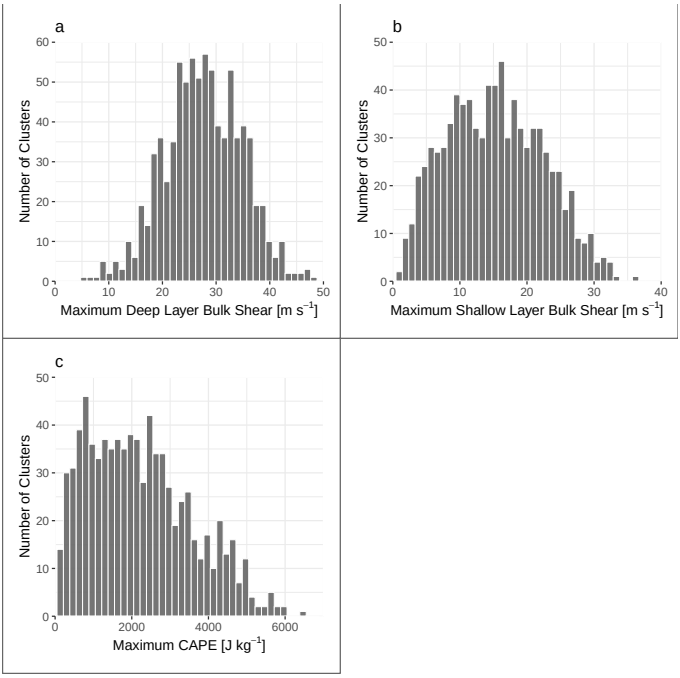

Fig. 5 Distribution of the environmental factors that are used as response variables in the model. DLBS and SLBS follow a normal distribution. CAPE is right-skewed with most clusters having less than 3000 J kg^{-1}.

of 0 J kg^{-1} for clusters with at least ten tornadoes (Table 1). The median value is 2045 J kg^{-1}. The mean value of CAPE for clusters with at least ten tornadoes is 2199 J kg^{-1}. In total, 53.98 % of clusters have less than the median value of CAPE. It is important to note that CAPE's median and mean values in clusters with at least ten tornadoes have similar values. These similarities are taken into account when fitting the CAPE model discussed below.

The explanatory variables in this research are a combination of physical and spatio-temporal variables (Table 1). The range of values for these variables is consistent with the literature. The average CSST is 27.6°C for the 830 clusters in this research. The average GAKSST is 7.51°C, and the average NinoSST is 29.6°C. The maximum standardized geopotential height difference for the NAO is 26.5 m and 36.7 m for the PNA.

Table 1 Variables considered in the regression models. Values include the maximum, minimum, and average across the 830 clusters with at least ten tornadoes.

Variable	Abbr	Max Value	Min Value	Avg Value
Explanatory Variables				
Latitude [° N]	ϕ	27.12	48.97	37.13
Longitude [° W]	λ	−109.9	−72.88	−92.00
Year	Y	1994	2020	2007
Caribbean SSTs (°C)	CSST	29.9	25.2	27.6
Gulf of Alaska SSTs (°C)	GAKSST	14.5	3.66	7.51
Nino 3.4 SSTs (°C)	NinoSST	31.5	27.6	29.6
North Atlantic Oscillation (m [sd])	NAO	2.65	−2.95	−0.0226
Pacific North American (m [sd])	PNA	3.67	−4.65	−0.209
Madden-Julian Oscillation (amplitude)	MJO	3.20	0.268	1.30
Response Variables				
Convective Available Potential Energy [J kg^{-1}]	CAPE	6530	0	2199
Deep Layer Bulk Shear [m s^{-1}]	DLBS	47.94	5.587	27.60
Shallow Layer Bulk Shear [m s^{-1}]	SLBS	35.72	1.085	15.24

Although each of these variables influences tornado frequency in the US, collinearity exists between the climate variables. There is a strong correlation between the GAKSST and CSST at a value of 0.897. Therefore, I compute the gradient between the SSTs (SSTgradient) by subtracting the maximum GAKSST from the maximum CSST for all clusters with ten or more tornadoes. After calculation of the SSTgradient, no collinearity issues remain between the climate variables (Fig. 6).

Regression Models

I fit a series of regression models to the cluster-level environmental data. Each environmental variable has a single model. The regression models quantify the effect of each climate factor on the environmental factors (CAPE, DLBS, SLBS) while holding the other variables constant. The random effects (an offset to the intercept term) in the model are the seasonal and hourly variability of the environmental factors. The climate variables for each cluster are the fixed effects in the models. The environmental factors for each cluster are the response variables in the models.

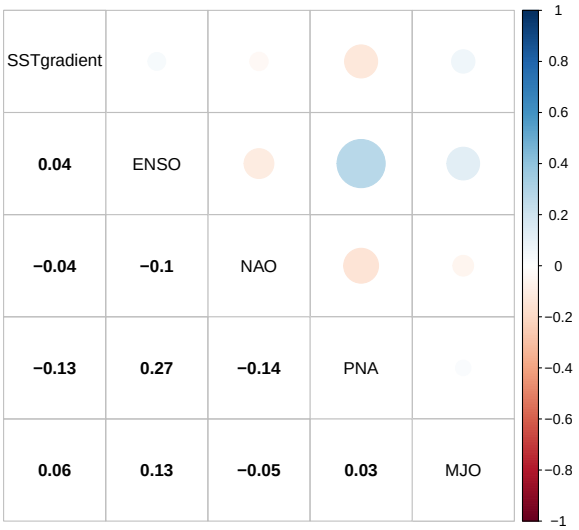

Fig. 6 A correlation plot of the climate variables used in the models. Blue dots indicate a positive relationship between the covariates. Red dots indicate a negative relationship between the covariates. The size of each dot highlights the magnitude of these relationships.

I fit a series of linear regression models to the data having the initial form

$$\begin{aligned} y = \quad & \beta_0 + \beta_\phi \phi + \beta_\lambda \lambda + \beta_Y Y + \beta_{\text{SSTgradient}} \text{SSTgradient}_i \\ & \beta_{\text{NinoSST}} \text{NinoSST}_i + \beta_{\text{NAO}} \text{NAO}_i + \beta_{\text{PNA}} \text{PNA}_i + \beta_{\text{MJO}} \text{MJO}_i + \\ & \beta_{\text{Hour}}(1|\text{Hour}_i) + \beta_{\text{Month}}(1|\text{Month}_i) + \epsilon_i, \end{aligned} \tag{1}$$

where the cluster center location [latitude (ϕ) and longitude (λ)], year (Y), and the five climate variables (SSTgradient, NINOSST, NAO, PNA, and MJO) are the explanatory variables in the model. The random effects in the model are month and hour. Therefore, β_{Month} and β_{Hour} are vectors of coefficients with one element for each month of the year and hour of the day. The coefficients

are computed using the maximum likelihood approach with the `lmer` function from the `lme4` package in R (Bates et al, 2015). I do the same for the initial SLBS and CAPE models. I simplify the initial models through single-term deletion described below.

I evaluate model skill by comparing the observed DLBS, SLBS, and CAPE with estimated values from the model. I obtain these values for each cluster by plugging the values of the explanatory variables into the final model. Predicted rates are under dispersed relative to the observed environmental factors. Comparisons are made using the Pearson correlation coefficient and mean absolute error. I evaluate the predictive skill of the models using in-sample and out-of-sample predictions. To compute the in-sample predictions, I fit a single model using the 830 clusters. To compute the out-of-sample predictions, I conduct a hold-one-out cross-validation [see (Elsner and Schmertmann, 1994)] where one cluster is held out of the model fitting procedure, and the model then uses that cluster to predict the environmental factors.

Deep-layer bulk shear model

I use data from the 830 clusters to regress DLBS onto the climate variables given in Table 1. The regression model quantifies the effect of these climate variables on DLBS while holding the other variables constant. The random effect in the model is the month because of the significant seasonal variation in DLBS. Climate variables are the fixed effects in the model, as are the latitude (Lat) and longitude (Lon) of the centroid for each cluster. I include Lat and Lon in the model to account for the spatial variability in DLBS values.

I add the fifteen-day averages of each climate variable to the initial model (Table 2). Climate variables with large t-values remain in the final model. The null hypothesis is rejected if the t-value on the coefficient estimate is greater

than 1. The null hypothesis cannot be rejected for the MJO, NinoSST, and year in the initial DLBS model. All significant climate variables have signs on the coefficients that are physically reasonable (Table 2). DLBS increases for an increase in the SSTgradient. DLBS also increases for every degree N and degree E increase in Lat and Lon, respectively.

Table 2 Coefficients in the DLBS model. The initial model is simplified through single-term deletion to achieve the model with the lowest AIC.

Coefficient	Estimate	S.E.	t value
	Initial Model		
β_0	-40.0	57.2	-0.700
β_ϕ	0.346	0.0604	5.72
β_λ	0.149	0.035	4.296
β_Y	0.0212	0.0288	0.736
β_{NAO}	-0.881	0.272	-3.24
β_{PNA}	-0.581	0.207	-2.81
β_{MJO}	-0.172	0.406	-0.423
$\beta_{NinoSST}$	0.287	-0.318	0.902
$\beta_{SSTgradient}$	0.981	0.271	4.51
	Final Model		
β_0	11.9	5.32	2.24
β_ϕ	0.344	0.0602	5.72
β_λ	0.148	0.0344	4.30
β_{NAO}	-0.880	0.270	-3.25
β_{PNA}	-0.548	0.202	-2.72
$\beta_{SSTgradient}$	0.884	0.203	4.34

All variables in the final DLBS model are significant. This regression model is best as it has the lowest Akaike Information Criterion (AIC) score, which measures the goodness of fit for the model. The in-sample correlation between the observed DLBS values and the predicted values is r = 0.565 [0.52, 0.61, 95% confidence interval (CI)]. The model statistically explains 36.3% of the variation in cluster-level DLBS but tends to over predict DLBS for clusters with lower observed DLBS values and slightly under predict DLBS for larger values of observed DLBS (Fig. 7). The conditional standardized residuals between the actual and model estimated values of DLBS follow a normal distribution which indicates an adequate model.

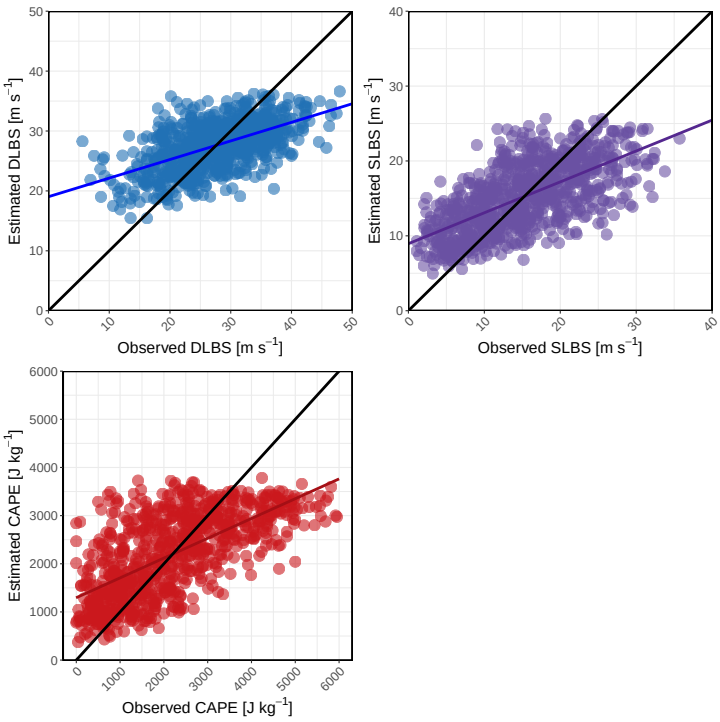

Fig. 7 Actual versus estimated DLBS, SLBS, and CAPE for clusters with at least ten tornadoes using their respective models. DLBS is blue, SLBS is purple, and CAPE is red. The points on the graph tend to fall along a line from lower left to upper right but with a slope less than one.

The model coefficients on the climate variables are consistent with expectations given recent literature. Specifically, DLBS increases for increasing Lat, Lon, and SSTgradient and decreases for increasing NAO and PNA. Latitude is the most important fixed effect in the model, as seen by its corresponding t-value. Quantitatively, the coefficient on the NAO term indicates that DLBS decreases by 0.880 m s^{-1} for every 1 m increase in the standard deviation of the NAO. A positive NAO is known to limit severe convective weather in the US. The coefficient on the PNA term indicates that DLBS decreases by 0.548 m s^{-1} for every 1 m increase in the standard deviation of the PNA. A positive PNA results in a weaker geopotential height gradient over North America, limiting shear. The coefficient on the SSTgradient term indicates that DLBS

increases by 0.884 m s^{-1} for every 1° increase in the SSTgradient holding the other variables constant. This result indicates that the more substantial differences in SSTs between the Caribbean and Gulf of Alaska, the stronger the association with DLBS for days with clusters of at least ten tornadoes. For every 1°N increase in Lat, DLBS increases by 0.34 m s^{-1} holding the other variables constant. This result is consistent with expectations because the jet stream influences upper-level winds and plays a crucial role in shear in the higher latitudes. For every 1°E increase in Lon, DLBS increases by 0.15 m s^{-1} holding the other variables constant. This result is consistent with other researchers who indicate that DLBS values are higher in the Southeast (Sherburn and Parker, 2014).

Shallow-layer bulk shear model

Similar to the DLBS model, a regression model is fit to SLBS using the same explanatory variables Table 1. A substantial seasonal variation also characterizes SLBS, so the month is included in the model as a random effect. Climate variables are the fixed effects in the model, as are the Lat and Lon of the centroid for each cluster. I include Lat and Lon in the model to account for the spatial variability in SLBS values.

I add the fifteen-day averages of each climate variable to the initial SLBS model consistent with the DLBS model (Table 3). Climate variables with large t-values remain in the final SLBS model. For the SLBS model, the null hypothesis cannot be rejected for the MJO and NinoSST. The year is significant in the model, indicating a positive and significant annual upward trend in SLBS on average independent of the other variables. All significant climate variables have signs on the coefficients that are physically reasonable (Table 3). SLBS increases with increasing SSTgradient and longitude eastward.

Table 3 Coefficients in the SLBS model. The initial model is simplified through single-term deletion to achieve the model with the lowest AIC.

Coefficient	Estimate	S.E.	t value
	Initial Model		
β_0	-140	52.6	-2.67
β_ϕ	-0.158	0.055	-2.85
β_λ	0.385	0.032	12.1
β_Y	0.093	0.027	3.50
β_{NAO}	-0.378	0.250	-1.51
β_{PNA}	-0.570	0.191	-2.99
β_{MJO}	0.236	0.374	0.632
$\beta_{NinoSST}$	-0.019	0.290	-0.065
$\beta_{SSTgradient}$	0.613	0.193	3.18
	Final Model		
β_0	-140	52.4	-2.66
β_ϕ	-0.157	0.055	-2.85
β_λ	0.384	0.032	12.1
β_Y	0.092	0.026	3.59
β_{NAO}	-0.385	0.249	-1.55
β_{PNA}	-0.570	0.186	-3.07
$\beta_{SSTgradient}$	0.615	0.183	3.36

All variables in the final SLBS model are significant. The final regression model has the lowest Akaike Information Criterion (AIC) score, which measures the trade-off between fit and overfitting. The in-sample correlation between the observed SLBS values and the predicted values is r = 0.648 [0.61, 0.69, 95% uncertainty interval (UI)]. The model statistically explains almost 37.6% of the variation in cluster-level SLBS but tends to over predict SLBS for clusters with lower observed SLBS values and slightly under predict SLBS for larger values of observed SLBS (Fig. 7). The conditional standardized residuals between the actual and estimated values of SLBS follow a normal distribution indicating an adequate model.

The model coefficients on the climate variables are consistent with expectations given recent literature. Specifically, SLBS increases for increasing Lon, Year, and the SSTgradient and decreases for increasing Lat, NAO, and PNA. Year is the most important fixed effect in the model, as seen by its corresponding t value. The coefficient on the NAO term indicates that SLBS decreases by 0.385 m s^{-1} for every 1 m increase in the standard deviation of the NAO. The

coefficient on the PNA term indicates that SLBS decreases by 0.570 m s^{-1} for every 1 m increase in the standard deviation of the PNA. A positive PNA leads to a weaker height gradient over North America, which reduces shear. The coefficient on the SSTgradient term indicates that SLBS increases by 0.615 m s^{-1} for every 1° increase in the SSTgradient holding the other variables constant. This result indicates that the more substantial differences in SSTs between the Caribbean and Gulf of Alaska, the stronger the association with SLBS for days with clusters of at least ten tornadoes. For every 1°N increase in Lat, SLBS decreases by 0.157 m s^{-1} holding the other variables constant. For every 1°E increase in Lon, SLBS increases by 0.38 m s^{-1} holding the other variables constant. This result is consistent with the literature (Sherburn and Parker, 2014) which indicate that SLBS values are higher in the southeastern US. SLBS is decreasing annually at a rate of 0.092 m s^{-1} holding the other variables constant.

Convective available potential energy model

Finally, a regression model is fit to CAPE using the same explanatory variables (Table 1). The regression model quantifies the effect of these climate variables on CAPE while holding the other variables constant. The random effect terms in the CAPE model are the month and hour of the cluster because of the considerable seasonal and diurnal variation in CAPE. For this model, the climate variables are the fixed effects in the model, as are the Lat and Lon of the centroid for each cluster.

To remain consistent, the initial CAPE model uses only the fifteen-day averages of each climate factor (Table 4). Only climate variables with a large t-value remain in the final model consistent with the shear models. The null hypothesis cannot be rejected for the CAPE model for Year, Lat, NinoSST,

NAO, and PNA. All significant climate variables have signs on the coefficients that are physically reasonable (Table 4).

Table 4 Coefficients in the CAPE model. I simplify the initial models through single-term deletion to achieve the model with the lowest AIC.

Coefficient	Estimate	S.E.	t value
	Initial Model		
β_0	-4217	10130	-0.416
β_ϕ	-8.12	11.0	-0.737
β_λ	-39.9	6.49	-6.14
β_Y	2.63	5.11	0.516
β_{NAO}	-7.95	48.0	-0.166
β_{PNA}	-33.1	36.7	-0.902
β_{MJO}	-108	71.6	-1.50
$\beta_{NinoSST}$	-46.8	56.1	-0.834
$\beta_{SSTgradient}$	-67.5	38.7	-1.74
	Final Model		
β_0	-735	881	-0.834
β_λ	-39.3	6.44	-6.10
β_{MJO}	-116	71.0	-1.63
$\beta_{SSTgradient}$	-50.6	35.3	-1.44

All variables in the final CAPE model are significant. The final regression model is best as it has the lowest Akaike Information Criterion (AIC) score, which measures the skill of the model. The in-sample correlation between the observed CAPE values and the predicted values is 0.652 [0.61, 0.69, 95% uncertainty interval (UI)]. The model statistically explains almost 35.8% of the variation in cluster-level CAPE but tends to over predict CAPE for clusters with lower observed CAPE values and under predict CAPE for larger values of observed CAPE (Fig. 7).

The conditional standardized residuals between the actual and estimated CAPE values follow a normal distribution that indicates an adequate model (Fig. 8). However, it is essential to note that there is a more extensive spread in model estimates for larger values of CAPE. The spread depends on the month of occurrence with increased variability of CAPE values during the spring and summer months when more clusters occur over a larger spatial domain on average.

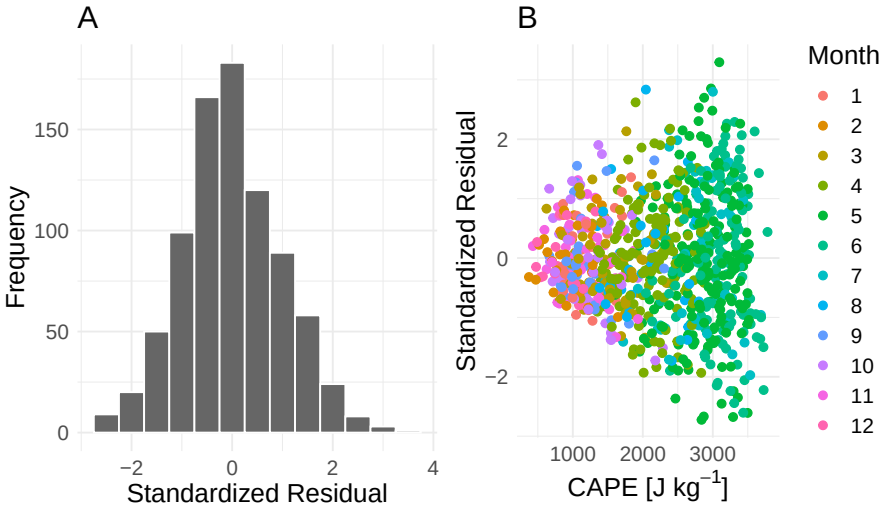

Fig. 8 Conditional standardized residuals from the linear regression model. (A) Histogram and (B) Residuals as a function of modeled estimated values of CAPE.

The model coefficients on the climate variables are consistent with expectations given recent literature. The coefficient on the MJO term indicates that CAPE decreases by 116 J kg^{-1} as the amplitude of the MJO increases by 1 m when holding the other variables constant. The coefficient on the SSTgradient term indicates that CAPE decreases by 50.6 J kg^{-1} for every 1° increase in the 15-day average SSTgradient holding the other variables constant. This result indicates that the more considerable the difference in SSTs between the Caribbean and Gulf of Alaska, the stronger the association with CAPE for days with clusters of at least ten tornadoes. For every 1°E increase in Lon, CAPE decreases by 39.3 J kg^{-1} holding the other variables constant. This result is consistent with other researchers who indicate that CAPE values are higher in the Great Plains region of the US (Sherburn and Parker, 2014; Dean and Schneider, 2012).

Sensitivity of the results to the averaging period

To directly test the sensitivity of the results to changes in the average period, I refit the models to include 10-day and 20-day averages instead of 15-day averages. The 10-day average climate variables do not improve the mean absolute error of the CAPE and DLBS models. The mean absolute error of the SLBS model is only marginally improved from 4.334 m s^{-1} to 4.327 m s^{-1} when using 10-day averages. The 20-day average climate variables do not improve the mean absolute error of the CAPE and SLBS models. The mean absolute error of the DLBS model is marginally improved from 4.67 m s^{-1} to 4.66 m s^{-1} when using 20-day average values of the climate variables. The sensitivity analysis provides evidence that the model results are not particularly sensitive to the temporal averages of the climate variables.

Model estimates

I illustrate the models by estimating the environmental factors using climate variables across a range of values that are significant in all three models (Lon and SSTgradient) (Fig. 9). I hold the explanatory variables for each model constant about their respective mean values. The year is set to 2020 for the SLBS model as it is only significant in this model. The random effects, month (all models) and hour (CAPE model only), are set to April and 18z due to maximum activity during the spring and evening hours. For a SSTgradient of 10°C and a Lon of 92°W, the models estimate DLBS to be 21 m s^{-}, SLBS to be 13 m s^{-1}, and CAPE to be 2364 J kg^{-1} using their respective models. For a SSTgradient of 25°C and a Lon of 72°W, the models estimate DLBS to be 37 m s^{-1}, SLBS to be 29.9 m s^{-1}, and CAPE to be 818 J kg^{-1} using their respective models. For a SSTgradient of 18°C and a Lon of 109°W, the models estimate DLBS to be 25.6m s^{-1}, SLBS to be 11.4 m s^{-1}, and

CAPE to be 2627 J kg^{-1} using their respective models. Figure 9 is a visual representation of the CAPE and DLBS fields when modeled over a range of values for the SSTgradient and Lon values. It is interesting to note that both shear models follow similar patterns where shear values increase for every 1°E shift in longitude and a 1°C increase in the SSTgradient. However, CAPE follows the opposite pattern where CAPE values decrease for every 1°E shift in longitude and increase the SSTgradient.

The SSTgradient is significant in all three models. An increased SSTgradient value leads to an increase in DLBS and SLBS with a decrease in CAPE. There is a clear distinction between the kinematic (wind-driven) and thermodynamic (temperature-driven) environmental factors. Increased shear is a result of the enhanced thermal wind caused by slope between the geopotential heights for a larger SSTgradient. The enhanced thermal wind leads to cooler temperatures which decrease CAPE values across the US. When the SST gradient between these two regions is smaller, the geopotential heights are similar, resulting in a decrease in shear. This decrease in the thermal wind leads to warmer temperatures which increase CAPE values across the US.

Discussion

The DLBS model highlights the spatial dependency and importance of the SSTgradient on DLBS values. DLBS covers the depth of the atmosphere extending from 1000 hPa to 850 hPa. The model indicates that DLBS values are larger in the southeastern US. High shear and low CAPE events tend to peak during the winter months and overnight, which is consistent with the climatology of tornadoes in the southeastern US (Sherburn and Parker, 2014; Sherburn et al, 2016; Grams et al, 2012). The model also indicates that DLBS values are larger in higher latitudes. The model result makes physical sense

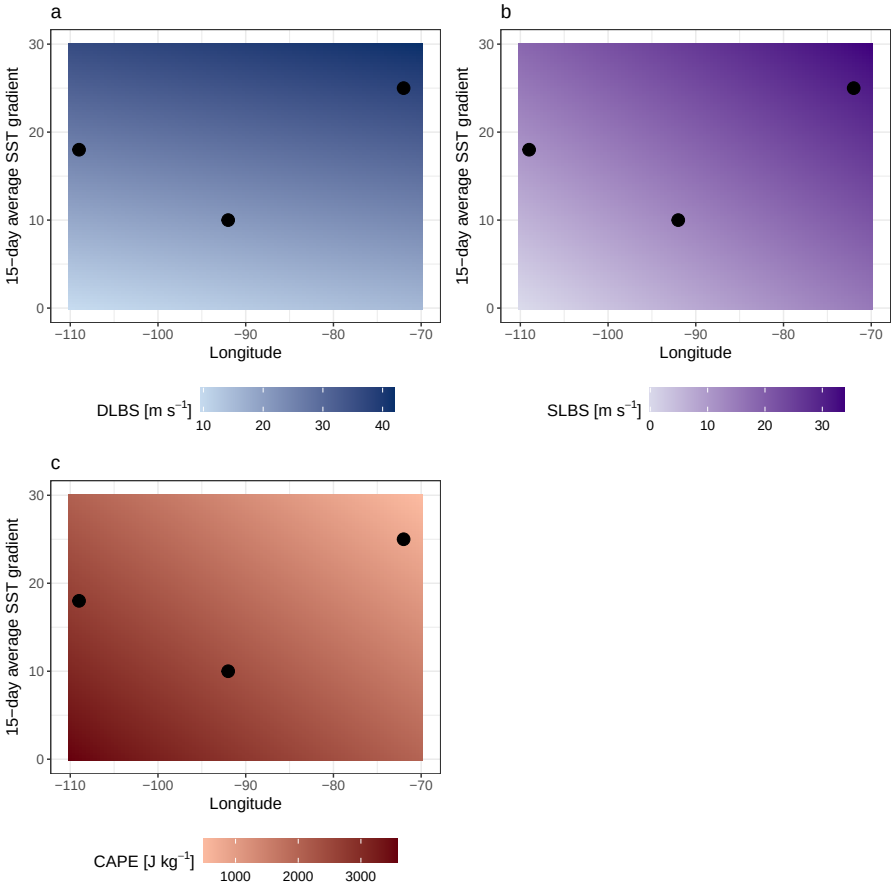

Fig. 9 Model estimates of DLBS (a), SLBS (b), and CAPE (c) across a range of Longitude and 15-day average SST gradient values holding the other explanatory variables constant at their mean value. For the CAPE model, I set the year to 2020. For the random effects, I set the month to April and Hour to 18Z. I calculate the estimates from the final regression models for each environmental factor.

because the jet stream can directly influence DLBS values. The larger the SSTgradient, the greater the DLBS as a result of the amplified thermal wind. Elsner and Widen (2014) show that tornado activity decreases with warmer Caribbean and Gulf of Alaska sea surface temperatures (Elsner and Widen, 2014). Therefore, increasing sea surface temperatures can weaken the gradient and decrease the DLBS values in the US, resulting in decreased tornado activity.

Additionally, the model indicates that DLBS values are dependent on the phase of the NAO and PNA. DLBS values decrease during the positive phase of the PNA. A positive PNA weakens the geopotential height gradient over the United States, which limits shear. Similarly, DLBS values decrease during the positive phase of the NAO. This finding is consistent with Elsner et al. (2016), who show that the phase of the NAO can limit severe convective weather in the US (Elsner et al, 2016b).

Similar to the DLBS model, SLBS values are spatially dependent and vary annually. The model indicates that SLBS values are larger in the southeastern US. Research consistently highlights larger shear values in the Southeast shown in the DLBS model (Sherburn and Parker, 2014; Sherburn et al, 2016; Grams et al, 2012). Additionally, the year term is significant in the model, indicating increasing SLBS values over time. This increase could be a result of the enhanced thermal wind caused by an increased SSTgradient as well as enhanced lower-level jets over North America (Weaver et al, 2012). The model indicates that a larger SSTgradient can lead to an increase of SLBS in the US. As shown above, tornado activity decreases when the SSTgradient is smaller (Elsner and Widen, 2014). However, low-level shear significantly influences severe convective weather in the US (Coffer and Parker, 2015; Weaver et al, 2012).

The CAPE model indicates that the values are dependent on the amplitude of the MJO, longitude, and SSTgradient. The MJO is a measure of convective energy near the equator. It takes roughly 2 to 5 weeks for these waves to transfer energy to higher latitudes. As such, CAPE values tend to increase with the increased convective energy caused by the MJO. Research has shown that CAPE values are lower in the Southeast as a result of increased moisture advection from the Gulf of Mexico (Sherburn and Parker, 2014; Sherburn et al,

2016; Grams et al, 2012). Moisture advection impacts these values because increased moisture at the mid-levels decreases the rate of environmental cooling. Finally, CAPE values decrease with an increased SSTgradient because it is temperature-dependent. Increased temperatures lead to large values of moisture in the boundary layer leading to an increase in CAPE values (Brooks, 2013; Diffenbaugh et al, 2008; DelGenio et al, 2007).

It is interesting to note that the NinoSST is not a significant predictor in any environmental models. Numerous studies highlight the significance of ENSO on tornado environments at the seasonal and subseasonal scales resulting from the physical mechanics of the jet stream (Molina et al, 2018; Lee and Galway, 1956; Ropelewski and Halpert, 1986; Cook and Schaefer, 2008; Allen et al, 2015a). Many of these studies focus on tornado activity's spatial and temporal distribution due to the ENSO phase. For example, Molina et al. (2018) found that tornado activity increases in the Southeast in the winter months when the ENSO phase is positive and increases in the Midwest in the summer months when the ENSO phase is negative (Molina et al, 2018). The current research focuses on the tornado environments at the cluster scale over a single convective day and climate variables 15-days prior to the cluster. The distinction in the spatial and temporal distributions between current and past research leads to a diluted influence of NinoSSTs on CAPE, DLBS, and SLBS. However, more work should focus on the influence of NinoSSTs on tornado environments at the cluster level.

The model results highlight the importance of understanding the role of climate variables on environmental factors for clusters with ten or more tornadoes. These results provide new information that can enhance the understanding of climate change on tornado environments when added to current research. For example, researchers have highlighted the increase in CAPE in a

warmer world (Elsner et al, 2014, 2018; DelGenio et al, 2007; Hoogewind et al, 2017; Brooks, 2013; Trapp et al, 2007). To date, this increase is attributed to increased moisture in the boundary layer as a result of increased sea surface temperatures (Brooks, 2013; Diffenbaugh et al, 2008; DelGenio et al, 2007). The CAPE model contributes to this understanding by showing that the weakened SSTgradient can also cause an increase in CAPE.

Additionally, shear values are projected to decrease as a result of a weakened temperature gradient between the equator and the poles (Brooks, 2013; Diffenbaugh et al, 2008). While this is true, the DLBS and SLBS models indicate that when the temperature gradient is larger, the US will experience larger deep and lower-level shear values conducive to tornado clusters with at least ten tornadoes. Therefore, localized increases in DLBS and SLBS remain a concern for enhanced convection in the future.

Conclusions

Tornado outbreaks are becoming more destructive on average. Recent studies indicate changes in environmental factors for tornadoes. This research focuses on the extent to which climate variables contribute to increases in CAPE and shear given an outbreak of at least ten tornadoes. It is important to note that I make no attempt to use climate variables to predict the occurrence of an outbreak. Instead, the study quantifies the conditional relationships between precursor SST and SLP variables and localized extremes of CAPE and shear when associated with outbreaks.

I use statistical models to quantify the relationship between environmental factors and climate variables for clusters with at least ten tornadoes. For this research, I extract CAPE, DLBS, and SLBS from the NARR dataset to represent the environment of clusters before the first tornado consistent with

previous research (Schroder and Elsner, 2019). I create a regression model for each environmental variable (response) to quantify its change due to climate variables (explanatory). Additional explanatory variables include location and year. As a result of the seasonal and diurnal variability of CAPE, DLBS, and SLBS, the random effects in the model are the month and hour.

The DLBS model explains 36.3% of the variation in cluster-level DLBS when using climate variables as explanatory variables. DLBS increases by 0.34 m s^{-1} for every 1°N increase in latitude, 0.15 m s^{-1} for every 1°E increase in longitude, and 0.88 m s^{-1} for every 1° increase in the SSTgradient. DLBS decreases by 0.88 m s^{-1} for a 1 m increase in the standard deviation of the NAO and 0.55 m s^{-1} for a 1 m increase in the standard deviation of the PNA. DLBS is location-dependent with the model indicating increased values in the North and East consistent with current literature (Sherburn and Parker, 2014; Sherburn et al, 2016). Additionally, DLBS increases with a stronger gradient between the Caribbean and Gulf of Alaska SSTs consistent with (Elsner and Widen, 2014).

The SLBS model explains 37.6% of the cluster-level variation in SLBS using the climate variables. The model indicates that SLBS increases by 0.38 m s^{-1} for every 1°E increase in longitude, 0.09 m s^{-1} each year, and 0.62 m s^{-1} for every 1° increase in the SSTgradient. SLBS decreases by 0.16 m s^{-1} for every 1°N increase in latitude, 0.57 m s^{-1} for a 1 m increase in the standard deviation of the PNA, and 0.39 m s^{-1} for a 1 m increase in the standard deviation of the NAO. SLBS is location-dependent with larger values in the South and East consistent with the literature (Sherburn and Parker, 2014; Sherburn et al, 2016).

The CAPE model explains 35.8% of the cluster-level variation in CAPE using the climate variables. The model indicates that CAPE decreases by 116

J kg^{-1} for a 1 m increase in the MJO, 50.6 J kg^{-1} for a 1° increase in the SSTgradient, and 39.3 J kg^{-1} for a 1°E increase in longitude. These results are consistent with the literature which suggests that lower values of CAPE are found in the Southeast (Gagan et al, 2010; Sherburn and Parker, 2014).

The models are a first step at understanding the influence of climate variables on environmental factors for clusters with at least ten tornadoes. These findings combined with previous research will aid in understanding the direct influence of climate variables on tornado outbreak characteristics, including tornado and casualty counts (Schroder and Elsner, 2021). For example, tornado and casualty counts may increase if the preceding climate variables increase DLBS when an outbreak occurs.

The focus on the last 25 years of a much longer tornado record is a limitation of this study. Considering additional tornado cases from earlier years could improve the study. However, including earlier years would lead to greater uncertainty on the estimates of clusters and the associated environmental factors. Additionally, NARR data tends to unrealistically favor environments for tornadoes in specific convective setups, which could affect the model results (Gensini and Ashley, 2011; Gensini et al, 2014; Allen et al, 2015b). Additional climate variables and variations in the temporal lag may also improve model performance. Specifically, utilization of the 5-month average ENSO may enhance model performance. Future work will examine how these environmental factors will influence tornado outbreak characteristics, including tornado and casualty counts.

Statements and Declarations

Funding

The author declares that no financial support was available for this work including but not limited to funds, grants, and other support.

Competing Interest

There is no relevant financial or non-financial interests to disclose.

Author Contribution

As the sole author, I am responsible for code development, analysis and interpretation of the results, and writing the manuscript.

Data Availability

The data is open-source and available through the National Oceanic and Atmospheric Administration. Data to fit all the models is available on GitHub (https://github.com/zschroder/tornenvir_climate).

Code Availability

All code used in this research was developed using the open-sourced program, R. The linear mixed effects models in this paper were implemented with the `lmer` function from the `lme4` R package (Bates et al, 2015). Graphics were made with the `ggplot2` (Wickham, 2017) and `tmap` (Tennekes, 2017) framework. The code and data to fit all the models is available on GitHub (https://github.com/zschroder/tornenvir_climate).

Ethics

The author has taken care to avoid any ethical violations that may impede her work.

Consent to Participate

I hereby consent to participate in the peer-review and publication processes set forth by this journal.

Consent for Publication

I hereby consent to pursue publication in this journal.

References

Allen JT, Tippett MK, Sobel AH (2015a) An empirical model relating U.S. monthly hail occurrence to large-scale meteorological environment. Journal of Advances in Modeling Earth Systems 7(1):226–243. https://doi.org/10.1002/2014MS000397, URL https://agupubs.onlinelibrary.wiley.com/doi/abs/10.1002/2014MS000397

Allen JT, Tippett MK, Sobel AH (2015b) Influence of the El Niño/Southern Oscillation on tornado and hail frequency in the United States. Nature Geosciences 8:278–283

Anderson-Frey AK, Richardson YP, Dean AR, et al (2018) Near-storm environments of outbreak and isolated tornadoes. Weather and Forecasting 33(5):1397–1412. https://doi.org/10.1175/WAF-D-18-0057.1, URL https://doi.org/10.1175/WAF-D-18-0057.1, https://arxiv.org/abs/https://doi.org/10.1175/WAF-D-18-0057.1

Baggett CF, Nardi KM, Childs SJ, et al (2018) Skillful subseasonal forecasts of weekly tornado and hail activity using the madden-julian oscillation. Journal of Geophysical Research: Atmospheres 123(22). https://doi.org/10.1029/2018jd029059, URL https://doi.org/10.1029/2018jd029059

Bates D, Mächler M, Bolker B, et al (2015) Fitting linear mixed-effects models using lme4. Journal of Statistical Software 67(1). https://doi.org/10.18637/jss.v067.i01

Brooks HE (2013) Severe thunderstorms and climate change. Atmos Res 123:129 – 138

Cheng V, Arhonditsis G, Sills D, et al (2015) A Bayesian modelling framework for tornado occurrences in North America. Nature Communications 6. https://doi.org/10.1038/ncomms7599

Chu JE, Timmermann A, Lee JY (2019) North American April tornado occurrences linked to global sea surface temperature anomalies. Science Advances 5(8):eaaw9950. https://doi.org/10.1126/sciadv.aaw9950, URL https://doi.org/10.1126/sciadv.aaw9950

Coffer BE, Parker MD (2015) Impacts of increasing low-level shear on supercells during the early evening transition. Monthly Weather Review 143(5):1945–1969. https://doi.org/10.1175/mwr-d-14-00328.1, URL https://doi.org/10.1175/mwr-d-14-00328.1

Cook AR, Schaefer JT (2008) The relation of El Niño-Southern Oscillation (ENSO) to winter tornado outbreaks. Monthly Weather Review 136:3121–3137

Cook AR, Leslie LM, Parsons DB, et al (2017) The Impact of El Niño–Southern Oscillation (ENSO) on Winter and Early Spring U.S. Tornado Outbreaks. Journal of Applied Meteorology and Climatology 56(9):2455–2478. https://doi.org/10.1175/JAMC-D-16-0249.1, URL https://doi.org/10.1175/JAMC-D-16-0249.1

Dean AR, Schneider RS (2012) P60 An examination of tornado environments, events, and impacts from 2003 - 2012. In: 26th Conference on Severe Local Storms

DelGenio AD, Yao MS, Jonas J (2007) Will moist convection be stronger in a warmer climate? Geophysical Research Letters 34(16). https://doi.org/10.1029/2007gl030525, URL https://doi.org/10.1029/2007gl030525

Diffenbaugh N, Trapp R, Brooks H (2008) Does global warming influence tornado activity? Eos, Transactions American Geophysical Union 89:553–554. https://doi.org/10.1029/2008EO530001

Doswell CA, Edwards R, Thompson RL, et al (2006) A simple and flexible method for ranking severe weather events. Weather and Forecasting 21(6):939–951. https://doi.org/10.1175/waf959.1, URL https://doi.org/10.1175/waf959.1

Elsner JB, Schmertmann CP (1994) Assessing forecast skill through cross validation. Weather and Forecasting 9(4):619–624

Elsner JB, Schroder Z (2019) Tornado damage ratings estimated with cumulative logistic regression. Journal of Applied Meteorology and Climatology 58(12):2733–2741. https://doi.org/10.1175/jamc-d-19-0178.1, URL https://doi.org/10.1175/jamc-d-19-0178.1

Elsner JB, Widen HM (2014) Predicting spring tornado activity in the central Great Plains by March 1st. Mon Wea Rev 142:259–267

Elsner JB, Murnane RJ, Jagger TH, et al (2013) A spatial point process model for violent tornado occurrence in the U.S. Great Plains. Mathematical Geosciences 45:667–679

Elsner JB, Jagger TH, Elsner IJ (2014) Tornado intensity estimated from damage path dimensions. PLoS ONE 9 (9):e107,571

Elsner JB, Elsner SC, Jagger TH (2015) The increasing efficiency of tornado days in the United States. Climate Dynamics 45(3-4):651–659

Elsner JB, Fricker T, Jagger TH, et al (2016a) Statistical models for predicting tornado rates: Case studies from Oklahoma and the Mid South USA. International Journal of Safety and Security Engineering 6:1–9

Elsner JB, Jagger TH, Fricker T (2016b) Statistical models for tornado climatology: Long and short-term views. PLoS ONE 11:e0131,090

Elsner JB, Fricker T, Schroder Z (2018) Increasingly powerful tornadoes in the United States. Geophysical Research Letters 46:392–398. https://doi.org/10.1029/2018GL080819

Forbes GS (2006) Meteorological aspects of high-impact tornado outbreaks. In: Preprints, 22nd Conf. on Severe Local Storms, Amer. Meteor. Soc., Hyannis, MA, pp 1–12

Fuhrmann CM, Konrad II CE, Kovach MM, et al (2014) Ranking of tornado outbreaks across the United States and their climatological characteristics. Weather and Forecasting 29:684–701

Gagan JP, Gerard A, Gordon J (2010) A historical and statistical comparison of "Tornado Alley" to "Dixie Alley.". National Weather Digest 34:145–155

Galway JG (1977) Some climatological aspects of tornado outbreaks. Monthly Weather Review 105:477–484

Gensini V, Ashley W (2011) Climatology of potentially severe convective environments from the North American Regional Reanalysis. Electronic Journal of Severe Storms Meteorology 6:1–40. https://doi.org/10.1038/s41612-018-0048-2

Gensini VA, Bravo de Guenni L (2019) Environmental covariate representation of seasonal U.S. tornado frequency. Journal of Applied Meteorology and Climatology 58(6):1353–1367. https://doi.org/10.1175/JAMC-D-18-0305.1, URL https://doi.org/10.1175/JAMC-D-18-0305.1

Gensini VA, Mote TL (2015) Downscaled estimates of late 21st century severe weather from CCSM3. Climatic Change 129(1-2):307–321. https://doi.org/10.1007/s10584-014-1320-z, URL https://doi.org/10.1007/s10584-014-1320-z

Gensini VA, Ramseyer C, Mote TL (2013) Future convective environments using NARCCAP. International Journal of Climatology 34(5):1699–1705. https://doi.org/10.1002/joc.3769, URL https://doi.org/10.1002/joc.3769

Gensini VA, Mote TL, Brooks HE (2014) Severe-thunderstorm reanalysis environments and collocated radiosonde observations. Journal of Applied Meteorology and Climatology 53(3):742–751. https://doi.org/10.1175/jamc-d-13-0263.1, URL https://doi.org/10.1175/jamc-d-13-0263.1

Gensini VA, Gold D, Allen JT, et al (2019) Extended u.s. tornado outbreak during late may 2019: A forecast of opportunity. Geophysical Research Letters 46(16):10,150–10,158. https://doi.org/10.1029/2019gl084470, URL https://doi.org/10.1029/2019gl084470

Gensini VA, Haberlie AM, Marsh PT (2020) Practically perfect hindcasts of severe convective storms. Bulletin of the American Meteorological Society 101(8):E1259–E1278. https://doi.org/10.1175/bams-d-19-0321.1, URL https://doi.org/10.1175/bams-d-19-0321.1

Grams JS, Thompson RL, Snively DV, et al (2012) A climatology and comparison of parameters for significant tornado events in the United States. Weather and Forecasting 27:106–123. https://doi.org/10.1175/WAF-D-11-00008.1

Heiss WH, McGrew DL, Sirmans D (1990) NEXRAD: next generation weather radar (WSR-88D). Microwave Journal 33(1):79

Hoogewind KA, Baldwin ME, Trapp RJ (2017) The impact of climate change on hazardous convective weather in the United States: Insight from high-resolution dynamical downscaling. Journal of Climate 30(24):10,081–10,100. https://doi.org/10.1175/JCLI-D-16-0885.1, URL https://doi.org/10.1175/JCLI-D-16-0885.1

Lee JT, Galway JG (1956) Preliminary report on the relationship between the jet at the 200-mb level and tornado occurrence. Bulletin of the American Meteorological Society 37(7):327–332. https://doi.org/10.1175/1520-0477-37.7.327, URL https://doi.org/10.1175/1520-0477-37.7.327

Lee SK, Atlas R, Enfield D, et al (2013) Is there an optimal ENSO pattern that enhances large-scale atmospheric processes conducive to tornado outbreaks in the United States? Journal of Climate 26:1626–1642

Lee SK, Wittenberg A, B Enfield D, et al (2016) US regional tornado outbreaks and their links to spring ENSO phases and North Atlantic SST variability. Environmental Research Letters 11:044,008. https://doi.org/10.1088/1748-9326/11/4/044008

Marsh PT, Brooks HE, Karoly DJ (2007) Assessment of the severe weather environment in north america simulated by a global climate model. Atmospheric Science Letters 8(4):100–106. https://doi.org/10.1002/asl.159, URL https://doi.org/10.1002/asl.159

Marzban C, Schaefer JT (2001) The correlation between US tornadoes and Pacific sea surface temperatures. Monthly Weather Review 129(4):884–895

Mercer AE, Shafer CM, Doswell CA, et al (2009) Objective classification of tornadic and nontornadic severe weather outbreaks. Monthly Weather Review 137(12):4355–4368. https://doi.org/10.1175/2009MWR2897.1

Mesinger F, DiMego G, Kalnay E, et al (2006) North American Regional Reanalysis. Bulletin of the American Meteorological Society 87(3):343–360. https://doi.org/10.1175/BAMS-87-3-343, URL https://doi.org/10.1175/BAMS-87-3-343, https://arxiv.org/abs/https://doi.org/10.1175/BAMS-87-3-343

Molina MJ, Allen JT, Gensini VA (2018) The gulf of mexico and ENSO influence on subseasonal and seasonal CONUS winter tornado variability. Journal of Applied Meteorology and Climatology 57(10):2439–2463. https://doi.org/

10.1175/jamc-d-18-0046.1, URL https://doi.org/10.1175/jamc-d-18-0046.1

Moore T (2017) On the temporal and spatial characteristics of tornado days in the United States. Atmospheric Research 184. https://doi.org/10.1016/j.atmosres.2016.10.007

Moore TW (2018) Annual and seasonal tornado trends in the contiguous United States and its regions. International Journal of Climatology 38:1582–1594. https://doi.org/10.1002/joc.5285

Moore TW, DeBoer TA (2019) A review and analysis of possible changes to the climatology of tornadoes in the united states. Progress in Physical Geography: Earth and Environment 43(3):365–390. https://doi.org/10.1177/0309133319829398, URL https://doi.org/10.1177/0309133319829398

Moore TW, Dixon RW, Sokol NJ (2016) Tropical cyclone Ivan's tornado cluster in the Mid-Atlantic region of the United States on 17–18 September 2004. Physical Geography 37(3-4):210–227. https://doi.org/10.1080/02723646.2016.1189299, URL https://doi.org/10.1080/02723646.2016.1189299

Rasmussen EN, Blanchard DO (1998) A baseline climatology of sounding-derived supercell and tornado forecast parameters. Weather and Forecasting 13(4):1148–1164. https://doi.org/10.1175/1520-0434(1998)013⟨1148:ABCOSD⟩2.0.CO;2, URL https://doi.org/10.1175/1520-0434(1998)013⟨1148:ABCOSD⟩2.0.CO;2

Ropelewski CF, Halpert MS (1986) North american precipitation and temperature patterns associated with the el niño/southern oscillation (ENSO). Monthly Weather Review 114(12):2352–2362. https://doi.org/10.

1175/1520-0493(1986)114⟨2352:napatp⟩2.0.co;2, URL https://doi.org/10.1175/1520-0493(1986)114⟨2352:napatp⟩2.0.co;2

Schneider RS, Brooks HE, Schafer JT (2004) Tornado outbreak day sequences: Historic events and climatology (1875–2003). In: Preprints,, 22nd Conf. on Severe Local Storms, Amer. Meteor. Soc., Hyannis, MA, pp 1–11

Schroder Z, Elsner JB (2019) Quantifying relationships between environmental factors and power dissipation on the most prolific days in the largest tornado "outbreaks". International Journal of Climatology https://doi.org/10.1002/joc.6388, URL https://doi.org/10.1002/joc.6388

Schroder Z, Elsner JB (2021) Estimating 'outbreak'-level tornado counts and casualties from environmental variables. Weather, Climate, and Society https://doi.org/https://doi.org/10.1175/WCAS-D-20-0130.1

Seeley JT, Romps DM (2015a) The effect of global warming on severe thunderstorms in the United States. Journal of Climate 28(6):2443–2458. https://doi.org/10.1175/JCLI-D-14-00382.1, URL https://doi.org/10.1175/JCLI-D-14-00382.1

Seeley JT, Romps DM (2015b) Why does tropical convective available potential energy (cape) increase with warming? Geophysical Research Letters 42(23):10,429–10,437. https://doi.org/10.1002/2015GL066199, URL https://doi.org/10.1002/2015GL066199

Shafer CM, Doswell CA (2011) Using kernel density estimation to identify, rank, and classify severe weather outbreak events. Electronic Journal of Severe Storms Meteorology 6:1–28

Sherburn KD, Parker M (2014) Climatology and ingredients of significant severe convection in high-shear, low-CAPE environments. Weather and Forecasting 29:854–877. https://doi.org/10.1175/WAF-D-13-00041.1

Sherburn KD, Parker M, R. King J, et al (2016) Composite environments of severe and nonsevere high-shear, low-CAPE convective events. Weather and Forecasting 31:1899–1927. https://doi.org/10.1175/WAF-D-16-0086.1

Tennekes M (2017) tmap: Thematic Maps. URL https://CRAN.R-project.org/package=tmap, r package version 1.10

Thompson RL, Edwards R, Hart JA, et al (2003) Close proximity soundings within supercell environments obtained from the Rapid Update Cycle. Weather and Forecasting 18(6):1243–1261. https://doi.org/10.1175/1520-0434(2003)018⟨1243:cpswse⟩2.0.co;2, URL https://doi.org/10.1175/1520-0434(2003)018⟨1243:cpswse⟩2.0.co;2

Tippett MK, Cohen JE (2016) Tornado outbreak variability follows Taylor's power law of fluctuation scaling and increases dramatically with severity. Nature Communications 7:10,668. https://doi.org/10.1038/ncomms10668

Tippett MK, Sobel AH, Camargo SJ (2012) Association of U.S. tornado occurrence with monthly environmental parameters. Geophysical Research Letters 39:L02,801

Tippett MK, Allen JT, Gensini VA, et al (2015) Climate and hazardous convective weather. Current Climate Change Reports 1(2):60–73. https://doi.org/10.1007/s40641-015-0006-6, URL https://doi.org/10.1007/s40641-015-0006-6

Tippett MK, Lepore C, Cohen JE (2016) More tornadoes in the most extreme U.S. tornado outbreaks. Science 354(6318):1419–1423. https://doi.org/10.1126/science.aah7393, URL https://doi.org/10.1126/science.aah7393

Trapp RJ, Diffenbaugh NS, Brooks HE, et al (2007) Changes in severe thunderstorm environment frequency during the 21st century caused by anthropogenically enhanced global radiative forcing. Proc Natl Acad Sci (USA) 104(50):19,719–19,723. https://doi.org/10.1073/pnas.0705494104

Weaver SJ, Baxter S, Kumar A (2012) Climatic role of North American low-level jets on U.S. regional tornado activity. Journal of Climate 25:6666–6683

Wickham H (2017) tidyverse: Easily Install and Load 'Tidyverse' Packages. URL https://CRAN.R-project.org/package=tidyverse, r package version 1.1.1